

Lattice-Code based Multiple Access for the Uplink: Algorithms and Optimization

Tao Yang, *Member, IEEE*, Fangtao Yu, Qiuzhuo Chen, Rongke Liu, *Senior Member, IEEE*, and Shanxiang Lyu

Abstract

This paper studies a lattice-code based multiple-access (LCMA) system. In the uplink, K users encode their messages with the same 2^m -ary *ring code* mapped to 2^m -PAM, belonging to the ensemble of *lattice codes*. Each user's signal is spread with its designated signature sequence, and all users transmit simultaneously. The receiver attempts to compute K independent streams of integer-combinations (ICBs) of the users' messages. For this, 1) we establish and solve a new “*bounded independent vectors problem*” (BIVP) which identifies a near-optimal set of coefficient vectors w.r.t. the ICBs, outperforming existing LLL and HKZ lattice reduction methods; 2) we put forth new non-linear and linear LCMA soft detection algorithms, which calculate the a posteriori probability w.r.t. the ICB over the lattice. The per-user complexity is of order no greater than $O(K)$, suitable for massive access of K being large. The soft detection outputs are forwarded to K ring-code decoders to recover the messages. With our developed techniques, LCMA is shown to support a significantly higher load of users and exhibits an improved frame error rate over state-of-the-art interleave-division multiple-access (IDMA) and sparse-code multiple-access (SCMA) schemes. Such advances are achieved with just parallel processing and K single-user decoding operations, avoiding the implementation issues of successive interference cancelation and iterative detection.

Index Terms

Multiple access, multi-user detection, multi-user MIMO, massive access, coded modulation, lattice-codes, compute-forward, physical-layer network coding, iterative decoding, soft detection

I. INTRODUCTION

The *multiple access* (MA) problem is about how to support K users' reliable communication within N resource blocks in time, frequency and spatial domains. For K being very large, it becomes a

This work is supported by the National Key R&D Program of China (No.2020YFB1807102 and No. 2022YFB2902604).

massive access problem that is essential to “ubiquitous massive connectivity” envisaged for 6G [1].

From 1G to 5G, the MA design was based on orthogonal transmission, where the users are allocated with non-overlapping frequency bands, separated time-slots, orthogonal spreading codes, orthogonal sub-carriers and independent beams, respectively [2]. Orthogonal transmission is fundamentally limited by the following: First, the number of supported users K is capped by the number of resource blocks N . Second, dynamic resource allocation is required to maintain the orthogonality, where the signaling cost skyrockets as K becomes large. This becomes a bottleneck for massive access. Third, despite the orthogonalization at the transmitters, the wireless channel induces signal distortion that can easily destroy the orthogonality. This invokes an orthogonality-restoring process that may subject to an unaffordable cost [3], [4].

Non-orthogonal MA (NOMA) allows collision of multiple users’ packets. As such, the number of users K can go beyond the number of resource blocks N [5]. Further, one can trade-in a higher K by reducing the peak rates of individual users, providing a high flexibility that are very much desired for ubiquitous MA [1]. Moreover, NOMA enables grant-free (GF) transmission, with which the signalling overhead incurred by dynamic resource allocation can be slashed, making it possible to realize massive access in 6G.

A pivotal issue of MA is how to deal with multi-user interference (MUI). Most existing NOMA schemes are based on *interference suppression* and *cancelation* that “reject” the MUI, as in power-domain NOMA with successive interference cancelation (SIC) and code-domain NOMA with iterative detection and decoding (IDD) [6]. In theory, the mechanism of rejecting MUI generally leads to a reduced system load K/N . In practice, such schemes are subject to issues that have prevented them from being implemented in 5G: 1) The power-domain NOMA with SIC is subject to a fundamental loss in achievable rate, while the processing delay and accumulation of error propagation become drastic as K increases. 2) Existing code-domain NOMA schemes require IDD, i.e., iterations between the multi-user detector and a bank of K channel-code decoders. In particular, IDD requires a strict matching between the multi-user detector and the decoders, following the principle of extrinsic information transfer (EXIT) [7]. As the system load K/N increases, the EXIT function of the multi-user detector varies, which would break the matching. This leads to a failure of convergence that destroys the functionality of IDD receiver. Moreover, typically $Q = 4$ to 10 IDD iterations are required, which amounts to Q multi-user detection operations implemented in serial, as well as QK channel-code decoding operations. This may result in a high processing delay and a complexity that may not be affordable.

A. Contributions

In this paper, we study a lattice-code based MA (LCMA) system, which is regarded as a practical embodiment of the notion of compute-forward MA [8]. In contrast to conventional NOMA schemes that reject MUI, LCMA embraces MUI by exploiting the mapping between the structure of K users' superimposed signal and the lattice space. This paper contributes to this subject by developing a package of techniques involving: 1) efficient nonlinear and linear soft detection algorithms, 2) optimization methods and 3) practical lattice coding for LCMA.

In the uplink, K users encode their messages with the same lattice-code. We put forth a simple yet powerful practical lattice coding technique, referred to as 2^m -ary *ring-coded modulation* (RCM), suitable for the mainstream 2^m -PAM or 2^{2m} -QAM signaling. Each user's code-modulated sequence undergoes a spreading process with its signature sequence. The resultant signals of K users are transmitted simultaneously.

For the receiver, we propose to identify the optimized mapping between the superposition of the K users' signals and the lattice-code space by solving a new *bounded independent vector problem* (BIVP). The solution to BIVP is optimal in the sense of mean square error (MSE), and outperforms existing Lenstra-Lenstra-Lovász (LLL) and Hermite Korkine-Zolotarev (HKZ) methods. A solution to the optimized spreading sequences is also presented.

We devise efficient LCMA soft detection algorithms to calculate the *a posteriori probability* (APP) w.r.t. the integer-combination (ICB) of users' messages. Both non-linear and linear soft LCMA detectors are explicitly studied. The non-linear soft detector goes beyond existing regularized integer-forcing method for the latticed-coded based system. The linear soft detector is carefully devised such that its per-user complexity is of order no greater than $O(K)$. The resultant APP streams are forwarded to K ring-code decoders which make decisions on the K ICBs in parallel, leading to the recovery of all users' messages.

We demonstrate that, without using SIC or IDD, LCMA can support a remarkably higher load of users, relative to existing state-of-the-art NOMA schemes. For example, with a 5G NR LDPC code of rate 1/2, LCMA achieves a system load of up to $K/N = 400\%$ in a fading MA channel, which dramatically outperforms baseline NOMA schemes such as IDMA and SCMA. Such advanced functionality and performance are achieved with low-latency parallel processing, low detection complexity of order less than $O(K)$ per-user, and exactly K channel-code decoding operations. These features would be desirable for MA and massive access in 6G systems. Beyond the uplink

MA setting, our developed techniques of LCMA can also be utilized for the downlink broadcast channel and distributed MIMO systems. Also, considerable performance improvement with the new non-linear soft detector over existing regularized integer-forcing is demonstrated.

B. Literature Review

1) *Multiple-access*: MA schemes that are based on interference cancelation and suppression have been extensively studied in the past two decades [4], [9]. Not long after the discovery of turbo codes in 1993, the “turbo principle” was introduced for the multi-user decoding, first by Wang&Poor [10]. Since 2000, turbo-like IDD has been extensively researched. In “turbo-CDMA” [10], the inner code is a multi-user detector with soft interference cancelation and linear minimum MSE (MMSE) suppression, while the outer code is a bank of K convolutional code decoders. Soft probabilities are exchanged among these components iteratively. In 2006, Li *et al.* introduced a chip-level interleaved CDMA, named after interleave-division multiple-access (IDMA) [11]. The chip interleaver enables uncorrelated chip interference, and thus a simple matched filter optimally combines the chip-level signal to yield the symbol-level soft information.

Low-density spreading CDMA and sparse-code MA (SCMA) differ from IDMA in that each symbol-level signal is spread only to a small number of chips, which forms a sparse matrix in the representation of the multi-user signal that can be depicted using a bi-partite factor graph [12]. SCMA also supports grant-free (GF) MA mode for the massive-connectivity scenario. Spatially coupled codes were also studied for dealing with the MA problem, yielding improved performance for fading MA channels thanks to the universality [13]. For IDMA and SCMA, spreading/sparse codes with irregular degree profiles were investigated including the work of ourselves [12], [14], which yielded improved convergence behavior of the multi-user decoding.

Rate-splitting MA (RSMA) was studied for closed-loop systems [15], [16]. The idea is to superimpose a common message on the private messages, which may enlarge the rate-region. Other code-domain NOMA techniques are proposed such as pattern division MA (PDMA), multi-user shared access (MUSA) and etc. [17], which exhibits merits for implementation. For grant-free MA, active user identification based on compressive sensing and coded slotted Aloha protocols are studied [18]–[20], which enables slashed signaling overhead that is essential to massive access. Here we are not able to list all existing results in the area of MA, and readers are encourage to refer to the excellent survey in [3]. Note that most existing MA schemes rely on the notion of “rejecting MUI”, where the MUI structure is not or insufficiently exploited.

2) *Literatures of Lattice-codes and Compute-forward*: For general multi-user networks, it has been proved that “structured codes” based on lattices can achieve a larger capacity region compared to conventional “random-like coding” [21]. The proof was based on the idea of “algebraic binning” of codewords, where each bin collects a certain subset of all codewords. The structure of lattice-codes enables efficient generation of the bin-indices as in the source coding with side information (SI) problem, and efficient decoding of the bin-indices as in the channel coding with SI problem [22]. For the physical-layer network coding (PNC) or compute-forward (CF) problem, by adopting lattice-codes at source nodes, the receiver can directly compute the bin-indices in the form of *integer-combinations* of all users’ messages [23], leading to remarkable coding gain or even multiplexing gain [24], [25]. The work in [26] extended the computation of single integer-combination in the original CF framework to simultaneous computation of more than one integer-combinations. The results on using lattice-codes for tackling MIMO detection and downlink MIMO precoding problems were reported in [27] and [28] under the name of integer-forcing (IF). The latter borrowed the notion of reverse CF which exploited the uplink-downlink duality [29], [30]. Various lattice reductions methods for identifying a “good” coefficient matrix for the integer-combinations have been reported in many works such as [31]. Recently, CF and IF have been extended to time-varying or frequency-selective fading channels using multi-mode IF and ring CF [32], [33]. The IF notion was also applied to solve the inter-symbol-interference equalization problem with the help of cyclic linear codes [34]. Here we are not able to list all existing results on lattice-codes, CF and IF, and highly motivated readers are encouraged to refer to [22] and [26].

3) *Lattice-codes and MA*: From an information theoretic perspective, Zhu and Gastpar showed that any rate-tuple of the entire Gaussian MA capacity region can be achieved using a lattice-code based approach, and the scheme was named compute-forward MA (CFMA) [8]. In contrast to random-like coding approaches exploited in existing NOMA schemes, lattice-code based MA exhibits greater capacity region achieved with low-cost single-user decoding. The design of CFMA for the Gaussian MA channel with binary codes was studied in [35]. Recently, we extend the result of [8] and [35] to fading MA channel with practical q -ary codes [36], [37].

To date, most of the related works on lattice-codes for MA have been focusing on achievable rates by proving the existence of “good” nested lattice-codes, whereas the practical aspects are not yet sufficiently researched. The works in [35] and [37] do not apply to practical 2^{2m} -QAM signaling and MIMO. The impacts of lattice-codes on the key performance indicators such as the system load, FER, latency, complexity and etc., remain not reported in the literature. In addition, for a large K , there

lacks efficient algorithms for both the soft detection and the identification of the coefficient matrix with realistic implementation costs. This motivates us to develop a package of practical coding, efficient signal processing algorithms and optimization methods for lattice-code based MA.

II. PRELIMINARIES OF LATTICE-CODES WITH RING-CODED MODULATION

This section presents the coding and modulation upon which LCMA is built. We suggest a simple yet powerful lattice code, namely 2^m -ary ring-coded modulation (RCM) with 2^m -PAM signaling, as the underlying coded-modulation for LCMA. RCM is much simpler than existing low-density lattice-codes [38], which does not apply to mainstream modulation schemes.

Let $\mathbf{b} = [b[1], \dots, b[k]]^T$ denote a q -ary message sequence¹. Each entry of \mathbf{b} belongs to an integer ring $\mathbb{Z}_q \triangleq \{0, \dots, q-1\}$. For a prime q , \mathbb{Z}_q becomes a Galois field $\text{GF}(q)$. For a non-prime q , e.g., $q = 2^m, m = 1, 2, \dots$, the addition and multiplication rules of \mathbb{Z}_{2^m} are *different* from those of $\text{GF}(2^m)$. This paper is primarily interested in $q = 2^m$ which matches with the mainstream 2^{2m} -QAM signaling.

A 2^m -ary ring-code with *generator matrix* \mathbf{G} of size n -by- k is employed to encode \mathbf{b} , given by

$$\mathbf{c} = \text{mod}(\mathbf{G}\mathbf{b}, 2^m) = \mathbf{G} \otimes \mathbf{b} \quad (1)$$

where “ \otimes ” represents the operation of matrix multiplication modulo- 2^m and $\mathbf{c} \in \mathbb{Z}_{2^m}^n$. Let \mathcal{C}^n denote the codebook collecting all 2^{mk} codewords w.r.t. (1). A random vector $\mathbf{d} \in \mathbb{Z}_{2^m}^n$ may be generated and added on \mathbf{c} for random permutation. For conciseness, the details are omitted, see [39], [40].

Each entry of \mathbf{c} is *one-to-one* mapped to a symbol that belongs to a constellation of 2^m points. For 2^m -PAM constellation (with identical spacing), the mapping is

$$\mathbf{x} = \delta(\mathbf{c}) = \frac{1}{\gamma} \left(\mathbf{c} - \frac{2^m - 1}{2} \right) \in \frac{1}{\gamma} \left\{ \frac{1 - 2^m}{2}, \dots, \frac{2^m - 1}{2} \right\}^n. \quad (2)$$

Here γ normalizes the average symbol energy. The rate of RCM is $R = \frac{k}{n} \log_2 q = \frac{km}{n}$ bits/symbol. For a complex-valued model, two independent 2^m -level RCM, one for the inphase part and the other for the quadrature part, form a RCM with 2^{2m} -QAM signaling. That is,

$$\begin{aligned} \mathbf{c}^{\text{Re}} &= \mathbf{G} \otimes \mathbf{b}^{\text{Re}}, \mathbf{c}^{\text{Im}} = \mathbf{G} \otimes \mathbf{b}^{\text{Im}}, \\ \mathbf{x} &= \left(\mathbf{c}^{\text{Re}} - \frac{2^m - 1}{2} \right) + j \left(\mathbf{c}^{\text{Im}} - \frac{2^m - 1}{2} \right). \end{aligned} \quad (3)$$

¹The conversion from a binary message sequence to a q -ary message sequence is straightforward.

Gaussian and Einstein integers for complex-valued model are beyond the scope of this paper [41].

Remark 1: [“Good” generator matrices \mathbf{G}] For $m = 1$, RCM reduces to binary channel coding with BPSK (or QPSK) signaling. Any state-of-the-art binary channel codes, such as LDPC codes and polar codes in 5G NR standards, can be utilized to execute (1) and the associated decoding. For $m = 2, 3, \dots$, repeat-accumulate ring-codes are studied in a separate work of ours [42]. By introducing a doubly irregular structure w.r.t. the *zero-divisors* of the integer ring, our developed 2^m -ary ring-codes approach the near-capacity of the 2^m -PAM input AWGN channels. Such codes are ready to be used in a LCMA system.

Remark 2: [RCM versus conventional coded-modulation] The RCM differs from conventional bit-interleaved coded-modulation (BICM), trellis coded-modulation (TCM) and multi-level coding with superposition coded-modulation (SCM) schemes. In those schemes, binary coded sequence \mathbf{c} is de-multiplexed into m streams $\mathbf{c}^{(1)}, \dots, \mathbf{c}^{(m)}$. Then, a *many-to-one* mapping given by $\mathbf{x} = \delta'(\mathbf{c}^{(1)}, \dots, \mathbf{c}^{(m)})$ is employed, e.g. the Grey mapping used for BICM. Due to the many-to-one mapping, such schemes do not belong to lattice-codes.

We next present the key property of RCM to be exploited in LCMA.

Property 1: For any K codewords $\mathbf{c}_1, \mathbf{c}_2, \dots, \mathbf{c}_K \in \mathcal{C}^n$, RCM satisfies

$$\sum_{i=1}^K a_i \mathbf{c}_i \in \tilde{\mathcal{C}}^n \quad (4)$$

for any integer-valued coefficients $[a_1, \dots, a_K]$, where $\tilde{\mathcal{C}}^n = \mathcal{C}^n + 2^m \dots \mathbb{Z}^n$ denotes the *extended codebook* by replicating the codewords in the base code \mathcal{C}^n over the infinite integer field \mathbb{Z}^n . Also,

$$\text{mod} \left(\sum_{i=1}^K a_i \mathbf{c}_i, 2^m \right) \in \mathcal{C}^n. \quad (5)$$

That is, the integer-sum of K codewords modulo- 2^m remains as a valid codeword.

Note that this property does not hold in conventional non-lattice coded based schemes such as BICM, TCM and SCM.

Remark 3: [Rings versus Galois Fields] Most existing works on lattice codes focused on prime q , where $\text{GF}(q)$ and \mathbb{Z}_q are equivalent. The integer additive property holds therein. In practical 2^m -PAM or 2^{2m} -QAM signaling, non-prime $q = 2^m$ is required. In this case, the integer additive property does not hold for coded-modulation based on $\text{GF}(2^m)$. To see this, recall that $\text{GF}(2^m)$ is an extension field of $\text{GF}(2)$, which has elements $\{0, 1, \beta, \beta^2, \dots, \beta^{2^m-2}\}$ [43]. The additive rule is determined based on the primitive element of the polynomials, which is different from the additive rule of integers as

in \mathbb{Z}_{2^m} . Therefore, to enable the integer additive property for 2^m -PAM signaling, the utilization of ring-codes over \mathbb{Z}_{2^m} is required.

Remark 4: [QAM vs. Gaussian signaling] RCM yields 2^m -PAM or 2^{2m} -QAM signaling, which is a mainstream modulation in practical systems. Compared to Gaussian signaling that is of interest in information theory, 2^m -PAM signaling enjoys easier treatment and low peak-to-average power ratio (PAPR), which are of high preference in practical uplink systems. The design of a practical shaping lattice to achieve the shaping gain (of at most 1.53 dB) is out of the scope of this paper.

III. SYSTEM MODEL AND UPLINK LCMA

Consider a single-cell MA system, i.e., without interference from other cells². The following assumptions are made for the clarity and conciseness of the model: 1) Each user is equipped with single-antenna and the BS is equipped with N_R antennas. The extension to multi-antenna users can be done by allowing multi-streams for each user as treated in [2]. 2) There is no inter-symbol-interference in the model, which can be ensured by adopting orthogonal frequency division multiplexing (OFDM)³. 3) This paper focus on presenting LCMA with a static fading model, where the channel coefficients remain unchanged for each coded block while differing over blocks. Our developed techniques can be extended to fast fading or frequency selective fading models by borrowing the notion of ring CF or multi-mode integer-forcing as treated in [32], [33].

Following the convention in studying uplink MA, we consider an open-loop system where there is no feedback to the transmitters to deliver the channel state information (CSI) or adaptive coding and modulation (ACM) information. Each user transmits at a target (symmetric) rate R_0 . The performance indicators of the uplink MA system are *system load* K/N and *frame error rate* (FER).

The problem under consideration is: how to design a transceiver architecture and efficient processing algorithms, such that the system supports a high system load K/N while the messages can be reliably decoded (i.e., a target FER is met), or achieves minimized FER for a given system load.

²Lattice-code based methods can also be developed for a multi-cell setup such as in distributed MIMO.

³The developed techniques may be extended to other advanced waveforms, but this is beyond the scope of this paper.

A. LCMA Transmitters

The architecture of a LCMA system is depicted in Fig. 1. K users encode their messages with the same⁴ 2^m -ary ring-code as in (1). Each user's encoded digits are one-to-one mapped to 2^m -PAM symbols as in (2), yielding *symbol-level* signal. The symbol-level signal of user i is multiplied with its designated spreading-signature sequence \mathbf{s}_i of length N_S , yielding the *chip-level* signals. Then all users transmit simultaneously.

For a real-valued model, the received signal is

$$\mathbf{Y} = \sum_{i=1}^K \sqrt{\rho} \mathbf{h}_i \mathbf{x}_i^T + \mathbf{Z} = \sqrt{\rho} \mathbf{H} \mathbf{X} + \mathbf{Z} \quad (6)$$

where ρ denotes the SNR, and \mathbf{Z} denotes the AWGN matrix whose entries are i.i.d with zero mean and unit variance. Note that \mathbf{H} denotes the transition matrix which is the aggregation of the length- N_S spreading sequences $\mathbf{s}_1, \dots, \mathbf{s}_K$ (in time or frequency domain) and the fading channel coefficient vectors of the N_R antennas (in spatial domain). The size of \mathbf{H} is N -by- K , where $N = N_R \times N_S$. A complex-valued model can be represented by a real-valued model of doubled dimension, i.e.,

$$\begin{bmatrix} \mathbf{Y}^{\text{Re}} \\ \mathbf{Y}^{\text{Im}} \end{bmatrix} = \sqrt{\rho} \begin{bmatrix} \mathbf{H}^{\text{Re}} & -\mathbf{H}^{\text{Im}} \\ \mathbf{H}^{\text{Im}} & \mathbf{H}^{\text{Re}} \end{bmatrix} \begin{bmatrix} \mathbf{X}^{\text{Re}} \\ \mathbf{X}^{\text{Im}} \end{bmatrix} + \begin{bmatrix} \mathbf{Z}^{\text{Re}} \\ \mathbf{Z}^{\text{Im}} \end{bmatrix} \quad (7)$$

as treated in [23], [44]. This paper presents with a real-valued model for clarity of presentation.

Compared to existing NOMA schemes, the distinguishing features of LCMA transmitter involve: a 2^m -ary ring-code (a lattice-code), a one-to-one 2^m -PAM mapping, and removal of the interleaver. Note that any spreading sequences developed for existing NOMA schemes can be used in LCMA.

Remark 5 (Grant-free Mode): LCMA supports GF mode, where the spreading sequence is replaced by random replicas as in coded slotted aloha (CSA) [19]. The receiver computes and stores the ICBs. Upon sufficient ICBs are accumulated in consecutive slots, a subset of the messages can be recovered.

B. LCMA Receiver

The receiver is set to compute K independent streams of *integer-combinations* (ICBs) of the users' messages, as shown in Fig. 1. The l th stream of *message-level* ICB is

$$\mathbf{u}_l^T \triangleq \text{mod} \left(\sum_{i=1}^K a_{l,i} \mathbf{b}_i^T, 2^m \right) = \mathbf{a}_l^T \otimes \mathbf{B}, l = 1, \dots, K, \quad (8)$$

⁴The extension to the asymmetric rate setup is straightforward. A low rate user's message, whose length is smaller than k , are zero-padded to form a length k message sequence. Then, the same channel code encoder can be utilize to encode all users' messages.

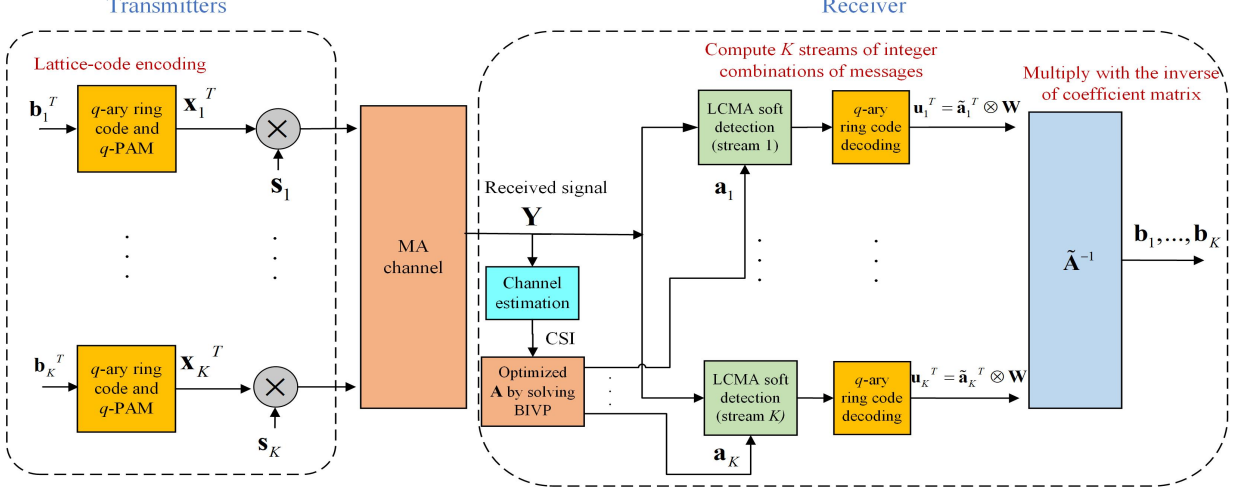


Fig. 1. Block diagram of the transmitters and receiver of a LCMA system. All users utilize the same 2^m -ary RCM. No interleavers and deinterleavers are used. For each fading MA channel realization, the optimized coefficient matrix \mathbf{A} is identified by solving the BIVP w.r.t. the channel state information. The LCMA soft detection and decoding of the K streams are implemented in parallel.

where $\mathbf{B} = [\mathbf{b}_1, \dots, \mathbf{b}_K]^T$, $\mathbf{a}_l = [a_{l,1}, \dots, a_{l,K}]^T$ has integer entries denoting the l th ICB *coefficient vector*.

Let $\mathbf{U} = [\mathbf{u}_1, \dots, \mathbf{u}_K]^T$ consist of all K streams of ICB. Let $\mathbf{A} = [\mathbf{a}_1, \dots, \mathbf{a}_K]^T$ stack up all K coefficient vectors, referred to as the *coefficient matrix*. Denote \mathbf{A} modulo- 2^m by $\tilde{\mathbf{A}} = \text{mod}(\mathbf{A}, 2^m)$, then

$$\mathbf{U} = \tilde{\mathbf{A}} \otimes \mathbf{B}. \quad (9)$$

It is required that $\tilde{\mathbf{A}}$ is of full rank K in \mathbb{Z}_{2^m} , thus it has a unique inverse $\tilde{\mathbf{A}}^{-1}$, i.e., $\tilde{\mathbf{A}}^{-1} \otimes \tilde{\mathbf{A}} = \mathbf{I}$. If all streams of ICBs $\mathbf{u}_1, \dots, \mathbf{u}_K$ are correctly computed, all K users' messages can be recovered by implementing

$$\mathbf{B} = \tilde{\mathbf{A}}^{-1} \otimes \mathbf{U}. \quad (10)$$

Here we study how to reliably compute $\mathbf{u}_1, \dots, \mathbf{u}_K$, where \mathbf{A} is given. The identification of the optimized \mathbf{A} will be studied in Section V. The optimal rule jointly computes $p(\mathbf{U}|\mathbf{Y})$. Since \mathbf{U} and \mathbf{B} are bijective, this is identical to computing $p(\mathbf{B}|\mathbf{Y})$, i.e., the joint multi-user decoding which is well-known to be formidable. A *parallel rule* for the K streams of ICBs computes

$$p(\mathbf{u}_l|\mathbf{Y}), l = 1, \dots, K, \quad (11)$$

which is used to approximate $p(\mathbf{U}|\mathbf{Y})$. The parallel rule can be enhanced by a successive rule [37]

$$p(\mathbf{u}_l|\mathbf{Y}, \mathbf{u}_1, \dots, \mathbf{u}_{l-1}), l = 1, \dots, K. \quad (12)$$

This paper focus on the parallel rule owing to its low-cost implementation, tractable analysis and optimization. Later we will see that the parallel rule yields competitive performance.

We now illustrate how to execute (11). Let $\mathbf{C} = [\mathbf{c}_1, \dots, \mathbf{c}_K]^T$ stack up all users' coded sequences generated by the 2^m -ary ring-code in (1). Define

$$\mathbf{v}_l^T \triangleq \text{mod} \left(\sum_{i=1}^K a_{l,i} \mathbf{c}_i^T, 2^m \right) = \mathbf{a}_l^T \otimes \mathbf{C}, \quad (13)$$

which is referred to as the l th stream of *codeword-level ICB*, $l = 1, \dots, K$.

Property 2: With the generator matrix \mathbf{G} in (1) and by applying Property 1, we have

$$\mathbf{v}_l = \text{mod} \left(\sum_{i=1}^K a_{l,i} \mathbf{G} \otimes \mathbf{b}_i, q \right) = \mathbf{G} \otimes \text{mod} \left(\sum_{i=1}^K a_{l,i} \mathbf{b}_i, 2^m \right) = \mathbf{G} \otimes \mathbf{u}_l. \quad (14)$$

That is, the codeword-level ICB and the message-level ICB are also related by generator matrix \mathbf{G} .

Property 2 allows for the computation of (11) by implementing:

- A *LCMA soft detector* calculates the symbol-wise a posteriori probabilities (APPs) w.r.t. the codeword-level ICB \mathbf{v}_l , written as $p(v_l[t] | \mathbf{y}[t])$, $t = 1, \dots, n$. Here $v_l[t]$ and $\mathbf{y}[t]$ denote the t -th column of \mathbf{v}_l and \mathbf{Y} .

- A *ring-code decoder* takes the APP as input and output a decision on the message-level ICB \mathbf{u}_l .

The above operations are executed in parallel for computing the ICBs $\mathbf{u}_1, \dots, \mathbf{u}_K$. Then, the messages of the K users are recovered by (10). Note that such treatment does not apply for non-lattice based MA schemes where Properties 1 and 2 do not hold.

Sections IV and IV of this paper are devoted to studying LCMA soft detectors. The details on the ring-code decoder can be found in [42].

IV. NONLINEAR SOFT DETECTION OF LCMA

In this section, we develop new nonlinear soft detection algorithms for LCMA. The new algorithms go beyond existing integer-forcing in terms of information rate, and apply to LCMA with a massive number of K .

A. Algebraic Binning and Multi-dimension PNC

For a given coefficient vector \mathbf{a}_l , a specific “*algebraic binning*” [23] structure is formed, explained below. Recall that each user's symbol belongs to a 2^m -PAM constellation. The superposition of the K users' symbols results a “*super-constellation*” of 2^{mK} *candidates*. For each ICB stream,

these 2^{mK} candidates are partitioned into 2^m “bins”. Those candidates with an identical ICB value $v_l[t] \triangleq \mathbf{a}_l^T \otimes \mathbf{c}[t] = \theta$, belong to the same bin of “bin-index” θ . The candidates with non-identical ICB values belong to different bins.

The soft detector attempts to compute the APPs of the bin-indices $p(v_l = \theta | \mathbf{y})$, $\theta = 0, \dots, 2^m - 1$, following the notion PNC (or CF). Since symbol-by-symbol detection is utilized, we omit the index “ t ” for the simplicity of notation. Using the Baye’s rule, we have

$$p(v_l = \theta | \mathbf{y}) = \frac{1}{\eta} \sum_{[x_1, \dots, x_K]^T: \mathbf{a}_l^T \otimes \mathbf{c} = \theta} p\left(\mathbf{y} \mid \sum_{i=1}^K \sqrt{\rho} \mathbf{h}_i x_i\right) = \frac{1}{\eta} \sum_{\mathbf{x}: \mathbf{a}_l^T \otimes \mathbf{c} = \theta} \exp\left(-\frac{\|\mathbf{y} - \sqrt{\rho} \mathbf{H} \mathbf{x}\|^2}{2}\right) \quad (15)$$

where η is to ensure that the APPs w.r.t. $\theta = 0, \dots, 2^m - 1$ add up to 1. Here the bijective mapping $c_i = \frac{1}{\gamma} \left(x_i + \frac{2^m - 1}{2}\right)$ in (2) is utilized. The calculation is based on the notion of PNC, and is performed in a N -dimension space. Thus, it is referred to as a “multi-dimension (MD) PNC” method.

Remark 6 (MD-PNC versus Integer-forcing): We note that MD-PNC is beyond integer-forcing (IF) [27]. Specifically, MD-PNC directly computes $p(v_l | \mathbf{y})$ over the *intact* N -dimension signal space. In contrast, IF applies linear filtering that forms a single-dimension signal space to compute the APP of v_l , as will be detailed in Section V. In fact, this may “overly compress” the signal space for computing the ICB. Due to data processing inequality [5], the MD-PNC method maintains a greater amount of information relative to the IF method.

In MD-PNC, the complexity of directly executing (15) with brute-force search has order $O(2^{mK})$, which is prohibitive. For a moderate size of K (e.g., $K < 16$), one may refer to a list sphere decoding (LSD) assisted method: given \mathbf{y} , apply the standard LSD [45] to form a list \mathcal{L} that contains the candidates that are within a certain radius to \mathbf{y} . Then, (15) is revised into

$$p(v_l = \theta | \mathbf{y}) = \frac{1}{\eta} \sum_{\mathbf{x} \in \mathcal{L}: \mathbf{a}_l^T \otimes \mathbf{c} = \theta} \exp\left(-\frac{\|\mathbf{y} - \sqrt{\rho} \mathbf{H} \mathbf{x}\|^2}{2}\right). \quad (16)$$

To obtain an accurate soft APP, the list size $|\mathcal{L}|$ has to be sufficiently large [45]. Empirically, it was suggested that $|\mathcal{L}|$ should be no smaller than 5-10% of the total number of candidates 2^{mK} . Yet, the complexity of LSD is exponential in $|\mathcal{L}|$, which quickly increases with K . Hence, the LSD assisted MD-PNC is still not ready to be utilized for a massive access setup with a large K .

B. Efficient Implementation of MD-PNC (Detection Method I)

We now propose an efficient way of realizing MD-PNC. For the l th ICB stream, let $\mathcal{I}_l \triangleq \{i : a_{l,i} \neq 0\}$ collect the positions of non-zero entries of \mathbf{a}_l , and let $\omega(\mathbf{a}_l) \triangleq |\mathcal{I}_l|$ denote the number

of non-zero entries of \mathbf{a}_l , referred to as its “weight”. Let \mathcal{I}_l^c denote the complementary set of \mathcal{I}_l . The received signal is then re-arranged into

$$\mathbf{y} = \sum_{i \in \mathcal{I}_l} \sqrt{\rho} \mathbf{h}_i x_i + \sum_{i \in \mathcal{I}_l^c} \sqrt{\rho} \mathbf{h}_i^T x_i + \mathbf{z} = \sum_{i \in \mathcal{I}_l} \sqrt{\rho} \mathbf{h}_i x_i + \boldsymbol{\xi}_l$$

The signals of the users with indices $i \in \mathcal{I}_l^c$ are regarded as irrelevant in computing the ICB v_l . The term $\boldsymbol{\xi}_l \triangleq \sum_{i \in \mathcal{I}_l^c} \sqrt{\rho} \mathbf{h}_i x_i^T + \mathbf{z}$ is the effective noise. In particular, $\boldsymbol{\xi}_l$ is a colored noise. We propose to perform a interference whitening processing for $\boldsymbol{\xi}_l$, using the following linear filter

$$\mathbf{T}_l = E (\boldsymbol{\xi}_l \boldsymbol{\xi}_l^T)^{-\frac{1}{2}} = \left(\sum_{i \in \mathcal{I}_l^c} \rho \mathbf{h}_i \mathbf{h}_i^T + \mathbf{I} \right)^{-\frac{1}{2}}. \quad (17)$$

The received signal then becomes

$$\tilde{\mathbf{y}}_l = \mathbf{T}_l \mathbf{y} = \sum_{i \in \mathcal{I}_l} \sqrt{\rho} \mathbf{g}_i x_i + \tilde{\mathbf{z}}_l, \quad (18)$$

for computing the l th stream of ICB. Here, the effective gain is $\mathbf{g}_i = \mathbf{T}_l \mathbf{h}_i$ and the whitened noise term is $\tilde{\mathbf{z}}_l = \mathbf{T}_l \boldsymbol{\xi}_l$ which now has i.i.d. entries with zero mean and variance 1.

Let \mathbf{c}^l consists of c_i , $i \in \mathcal{I}_l$. Let \mathbf{x}^l consists of x_i , $i \in \mathcal{I}_l$. The lengths of \mathbf{c}^l and \mathbf{x}^l are $\omega(\mathbf{a}_l)$. Using the Baye’s rule, the APP is calculated as

$$p(v_l = \theta | \tilde{\mathbf{y}}_l) \propto p(\tilde{\mathbf{y}}_l | \mathbf{a}_l^T \otimes \mathbf{c}^l = \theta) = \sum_{\mathbf{x}^l: \mathbf{a}_l^T \otimes \mathbf{c}^l = \theta} \exp\left(-\frac{\|\tilde{\mathbf{y}}_l - \sum_{i \in \mathcal{I}_l} \sqrt{\rho} \mathbf{g}_i x_i\|^2}{2}\right). \quad (19)$$

As such, the number of candidates related to the calculation of APP $p(v_l | \tilde{\mathbf{y}}_l)$ is reduced from 2^{mK} to $2^{m\omega(\mathbf{a}_l)}$. For the MA setup with a moderate K/N , the optimized ICB coefficient vectors have weights $\omega(\mathbf{a}_l)$, $l = 1, \dots, K$, much smaller than K with a high probability, for K and N being large. As such, the reduction in complexity is tremendous since $\omega(\mathbf{a}_l) \ll K$. Then, with the aid of standard LSD, the MD-PNC soft detection is ready to be utilized in a massive access setup with a large K .

C. Achievable Rate Analysis

Here we characterize the achievable rate of the LCMA scheme with a full list size of $|\mathcal{L}| = 2^{mK}$. Let X_i and V_l denote the random variables (R.V.s) of user i ’s transmitted signal and the l -th ICB, respectively. Let \underline{Y} denote the R.V. of the received signal vector of dimension N .

Theorem 1: For a given coefficient matrix \mathbf{A} of a unique inverse in \mathbb{Z}_{2^m} , an achievable rate region of K -user LCMA with parallel processing is characterized by

$$R_i^{(\mathbf{A})} \leq \log_2 2^m - \max_l \{\varphi(a_{l,i}) H(V_l | \underline{Y})\}$$

for $i = 1, \dots, K$, where

$$\varphi(a) = \begin{cases} 0, & a = 0 \\ 1, & a \neq 0 \end{cases},$$

and $H(\bullet)$ denotes the entropy function.

Proof. From Property 2, the probability of $V_l = \theta$ is given by

$$p(V_l = \theta) = \sum_{a_{11}j_1 \oplus \dots \oplus a_{l,K}j_K = \theta} \prod_{i=1}^K p(C_i = j_i) = \frac{2^{m(K-1)}}{2^{mK}} = \frac{1}{2^m}. \quad (20)$$

Therefore, $H(V_l) = H(X_i) = \log(2^m)$. For given \mathbf{A} , the achievable computation rate is [46]

$$R_{l,comp}^{(\mathbf{A})} \leq I(\underline{Y}; V_l), \quad l = 1, \dots, L,$$

where $I(\bullet)$ denotes the mutual information function. If $a_{l,i} \neq 0$, the l -th ICB V_l includes the message of user i , which implies that the rate of user i should be no greater than the achievable computation rate of the l -th integer-combination. Thus, the rate of user i satisfies

$$\begin{aligned} R_i^{(\mathbf{A})} &\leq \min_{l: a_{l,i} \neq 0} \{R_{l,comp}^{(\mathbf{A})}\} = \min_l \{H(V_l) - H(V_l|\underline{Y}) | a_{l,i} \neq 0\} \\ &\stackrel{(a)}{=} H(V_l) - \max_l \{H(V_l|\underline{Y}) | a_{l,i} \neq 0\} = \log_2 2^m - \max_l \{\varphi(a_{l,i})H(V_l|\underline{Y})\} \end{aligned}$$

where (a) follows from the fact that V_1, \dots, V_L are independently and uniformly distributed. ■

Corollary 1: A lower bound of the achievable symmetric rate of LCMA is given by

$$R_{sym}^{(\mathbf{A})} < \min_l \{\log_2 2^m - \varphi(a_{l,i})H(V_l|\underline{Y})\}, \quad (21)$$

which is simply the smallest of the achievable computation rates of all ICBs.

It can be shown that, for a given \mathbf{A} , the mutual information of MD-PNC is strictly greater than or equal to that of IF. This is due to that the signal-dimension compression in IF is avoided, leading to a greater achievable computation rate $R_{l,comp}^{(\mathbf{A})}$.

V. LINEAR SOFT DETECTION OF LCMA

In this section, we develop new linear soft detection algorithms for LCMA. The algorithms have per-user complexity no greater than $O(K)$, although they have inferior performance relative to the non-linear detection algorithms in general.

A. Linear Filtering and A Posteriori Probability (Detection Method II)

A linear LCMA soft detector first transforms the N -dimension received signal into K streams of single-dimension signals. Then, each stream is used to compute one ICB.

1) *Derivation of the exact APP (with any linear filter)*: Denote by \mathbf{W} a size K -by- N linear filtering matrix of real-valued entries. Let \mathbf{w}_l^T denote the l th row of \mathbf{W} , normalized to $\|\mathbf{w}_l\| = 1$. The l th filtered signal stream is

$$\tilde{\mathbf{y}}_l^T = \mathbf{w}_l^T \mathbf{Y} = \sqrt{\rho} \mathbf{w}_l^T \sum_{i=1}^K \mathbf{h}_i \mathbf{x}_i^T + \tilde{\mathbf{z}}_l^T. \quad (22)$$

Since symbol-by-symbol detection is utilized, we omit the time-index and the signal is expressed as

$$\tilde{y}_l = \sum_{i=1}^K \sqrt{\rho} \psi_{l,i} x_i + \tilde{z}_l \quad (23)$$

where $\psi_{l,i} = \mathbf{w}_l^T \mathbf{h}_i$ denotes the ‘‘effective gain’’ w.r.t. user i , and the noise term \tilde{z}_l has a unit variance.

Recall that $\mathcal{I}_l \triangleq \{i : a_{l,i} \neq 0\}$ collects the positions of non-zero entries of \mathbf{a}_l , and \mathcal{I}_l^c is the complementary set. Recall that $\omega(\mathbf{a}_l) \triangleq |\mathcal{I}_l|$ denotes the number of non-zero entries. Then, \tilde{y}_l is re-arranged as

$$\tilde{y}_l = \sum_{i \in \mathcal{I}_l} \sqrt{\rho} \psi_{l,i} x_i + \sum_{i \in \mathcal{I}_l^c} \sqrt{\rho} \psi_{l,i} x_i + \tilde{z}_l = \sum_{i \in \mathcal{I}_l} \sqrt{\rho} \psi_{l,i} x_i + \xi_l. \quad (24)$$

The term $\sum_{i \in \mathcal{I}_l} \sqrt{\rho} \psi_{l,i} x_i$ is the superposition of the signals of the $\omega(\mathbf{a}_l)$ users whose ICB coefficients are non-zero, which is the *useful signal* part. The term $\sum_{i \in \mathcal{I}_l^c} \sqrt{\rho} \psi_{l,i} x_i$ contains the signals of the remaining $K - \omega(\mathbf{a}_l)$ users whose ICB coefficients are zero, which can be regarded as irrelevant w.r.t. ICB. The term $\xi_l = \sum_{i \in \mathcal{I}_l^c} \sqrt{\rho} \psi_{l,i} x_i + \tilde{z}_l$ is treated as the *effective noise*, which is not correlated with the useful signal part.

Recall the one-to-one mapping $x_i = \frac{1}{\gamma} (c_i - \frac{2^m - 1}{2})$ in (2). For the clarity of presentation, we express the received signal with c_i (instead of with x_i), given as

$$\bar{y}_l = \gamma \tilde{y}_l + \frac{2^m - 1}{2} \sum_{i \in \mathcal{I}_l} \sqrt{\rho} \psi_{l,i} = \sum_{i \in \mathcal{I}_l} \sqrt{\rho} \psi_{l,i} \left(\gamma x_i + \frac{2^m - 1}{2} \right) + \gamma \xi_l = \sum_{i \in \mathcal{I}_l} \sqrt{\rho} \psi_{l,i} c_i + \bar{z}_l. \quad (25)$$

For a sufficiently large K , $|\mathcal{I}_l^c|$ is sufficiently large to apply Central Limit Theorem. Then $\bar{z}_l = \gamma \xi_l$ follows a Gaussian distribution with 0 mean and variance $\bar{\sigma}_l^2 = \gamma^2 (\rho \sum_{i \in \mathcal{I}_l^c} \psi_{l,i}^2 + 1)$.

Recall $\mathbf{v}_l \triangleq \mathbf{a}_l^T \otimes \mathbf{c}$. We abuse the notion be consider that \mathbf{c} only consists of $\{c_i, i \in \mathcal{I}_l\}$. With the above arrangement, the APP w.r.t. the l th ICB is now given by

$$p(v_l = \theta | \bar{y}_l) = \frac{1}{\eta} \sum_{\mathbf{c}: \mathbf{a}_l^T \otimes \mathbf{c} = \theta} p \left(\bar{y}_l | \sum_{i \in \mathcal{I}_l} \sqrt{\rho} \psi_{l,i} c_i \right) = \frac{1}{\eta} \sum_{\mathbf{c}: \mathbf{a}_l^T \otimes \mathbf{c} = \theta} \exp \left(- \left| \bar{y}_l - \sum_{i \in \mathcal{I}_l} \sqrt{\rho} \psi_{l,i} c_i \right|^2 / 2 \bar{\sigma}_l^2 \right), \quad (26)$$

where η is the normalization factor. The APP $p(v_l = \theta | \bar{y}_l)$ is equal to the sum of the likelihood functions of the $2^{m(\omega(\mathbf{a}_l) - 1)}$ candidates whose underlying ICB is equal to θ .

2) *Gaussian Approximation*: A direct execution of (26) requires to evaluate the Euclidean distances of $2^{m\omega(\mathbf{a}_l)}$ candidates of \mathbf{c} . Here we propose a low-complexity computation of (26). From the mechanism of PNC, there is a many-to-one mapping between $\mathbf{a}_l^T \mathbf{c}$ and $\mathbf{a}_l^T \otimes \mathbf{c}$ in general. Specifically, all the events $\{\mathbf{a}_l^T \mathbf{c} = \theta \pm \beta \cdot 2^m\}$ with various values $\bar{\theta} = \theta \pm \beta \cdot 2^m$ have an identical $\mathbf{a}_l^T \otimes \mathbf{c} = \theta$ after the modulo- 2^m operation. As such, using the Total Probability Rule, the APP is written as

$$p(v_l = \theta | \bar{y}_l) = \frac{1}{\eta} \sum_{\bar{\theta}: \text{mod}(\bar{\theta}, 2^m) = \theta} p(\bar{y}_l | \mathbf{a}_l^T \mathbf{c} = \bar{\theta}) p(\bar{\theta}). \quad (27)$$

Here we derive the likelihood function $p(\bar{y}_l | \mathbf{a}_l^T \mathbf{c} = \bar{\theta})$. Let $\Omega_l(\bar{\theta}) = \{\mathbf{c} : \mathbf{a}_l^T \mathbf{c} = \bar{\theta}\}$ collect the candidates \mathbf{c} with $\mathbf{a}_l^T \mathbf{c}$ equal to $\bar{\theta}$. The conditional mean for a given value of $\mathbf{a}_l^T \mathbf{c} = \bar{\theta}$ is

$$\mu_l(\bar{\theta}) = E_{\mathbf{c}}(\bar{y}_l | \mathbf{a}_l^T \mathbf{c} = \bar{\theta}) = E_{\mathbf{c}}\left(\sum_{i \in \mathcal{I}_l} \sqrt{\rho} \psi_{l,i} c_i + \bar{z}_l | \mathbf{a}_l^T \mathbf{c} = \bar{\theta}\right) = \frac{1}{|\Omega_l(\bar{\theta})|} \sum_{\mathbf{c} \in \Omega_l(\bar{\theta})} \sum_{i \in \mathcal{I}_l} \sqrt{\rho} \psi_{l,i} c_i. \quad (28)$$

The conditional variance is

$$\begin{aligned} \sigma_l^2(\bar{\theta}) &= E_{\mathbf{c}}\left(\left|\sum_{i \in \mathcal{I}_l} \sqrt{\rho} \psi_{l,i} c_i + \bar{z}_l - \mu_l(\bar{\theta})\right|^2\right) = E_{\mathbf{c}}\left(\sum_{i \in \mathcal{I}_l} \sqrt{\rho} \psi_{l,i} c_i\right)^2 - \mu_l^2(\bar{\theta}) + \gamma^2 \tilde{\sigma}_l^2 \\ &= \frac{1}{|\Omega_l(\bar{\theta})|} \sum_{\mathbf{c} \in \Omega_l(\bar{\theta})} \left(\sum_{i \in \mathcal{I}_l} \sqrt{\rho} \psi_{l,i} c_i\right)^2 - \mu_l^2(\bar{\theta}) + \gamma^2 \tilde{\sigma}_l^2. \end{aligned} \quad (29)$$

For a sufficiently large K , \bar{y}_l is well-approximated to have a conditional Gaussian distribution for all values of $\bar{\theta}$. With Gaussian approximation, the APP is then calculated as

$$p(v_l = \theta | \bar{y}_l) = \frac{1}{\eta} \sum_{\bar{\theta}: \text{mod}(\bar{\theta}, 2^m) = \theta} \exp\left(-\frac{(\bar{y}_l - \mu_l(\bar{\theta}))^2}{2\sigma_l^2(\bar{\theta})}\right) p(\bar{\theta}). \quad (30)$$

This is referred to as *Detection Method II*.

Here, the integer-valued $\bar{\theta}$ are within the range of $\bar{\theta} \in \left\{ \sum_{i: a_{l,i} < 0} a_{l,i} (2^m - 1), \dots, \sum_{i: a_{l,i} > 0} a_{l,i} (2^m - 1) \right\}$.

Define $\omega_H(\mathbf{a}_l) \triangleq \sum_{i \in \mathcal{I}_l} |a_{l,i}|$, referred to as the “weight” of \mathbf{a}_l . Then the cardinality of the set for $\bar{\theta}$ is precisely $\omega_H(\mathbf{a}_l) (2^m - 1) + 1$. In other words, there are $\omega_H(\mathbf{a}_l) (2^m - 1) + 1$ Euclidean distances needs to be calculated in (30). This is far less than $2^{m\omega(\mathbf{a}_l)}$ required in direct execution of (26).

For all K ICBS, the total amount of Euclidean distance calculations is

$$(2^m - 1) \sum_{l=1}^K \omega_H(\mathbf{a}_l) + K \leq 2^m \sum_{l=1}^K \omega_H(\mathbf{a}_l) = 2^m K \cdot E_{\mathbf{a}}(\omega_H(\mathbf{a})) \quad (31)$$

where $E_{\mathbf{a}}(\omega_H(\mathbf{a}))$ is the average weight of coefficient vectors. The average per-user complexity has order $O(2^m E_{\mathbf{a}}(\omega_H(\mathbf{a})))$. This is $E(\omega_H(\mathbf{a}))$ times of the complexity of single-user detection. As we will see in the next section, $E_{\mathbf{a}}(\omega_H(\mathbf{a}))$ is just a fraction of K in general.

3) *Details on the statistics:* Detection Method II requires a) the a priori probability $p(\bar{\theta})$, b) the conditional mean $\mu_l(\bar{\theta})$ and c) conditional variance $\sigma_l^2(\bar{\theta})$ (30), to be detailed below. Since these statistics are required to be calculated once per-block, the cost is minor compared to that in (30) which are computed n times per-block. For notational simplify, the index l is omitted in this part.

a) Let $n_1[\bar{\theta}] = 1$ for $\bar{\theta} = 0, a_1, \dots, (2^m - 1)a_1$ if $a_1 > 0$, and $\bar{\theta} = (2^m - 1)a_1, \dots, 0$ if $a_1 < 0$. Let $n_1[\bar{\theta}] = 0$ for the rest values of $\bar{\theta}$. Then $p(\bar{\theta})$ can be obtained by sequentially implementing

$$n_k[\bar{\theta}] = \sum_{\tau=0, \dots, 2^m-1} n_{k-1}[\bar{\theta} - a_i\tau] \quad (32)$$

until layer $K' = \omega(\mathbf{a})$ is reached. This requires no more than

$$\sum_{k=1}^{K'} (\omega_H([a_1, \dots, a_k]) (2^m - 1) + 1) (2^m - 1) \approx \sum_{k=1}^{K'} \omega_H([a_1, \dots, a_k]) (2^m - 1)^2$$

additions in total and does not involve multiplication.

b) The conditional means can be obtained by sequentially implementing

$$\tilde{\mu}_k[\bar{\theta}] = \sum_{\tau=0, \dots, 2^m-1} \tilde{\mu}_{k-1}[\bar{\theta} - a_i\tau] + \tau\sqrt{\rho}\psi_k. \quad (33)$$

When reaching layer $K' = \omega(\mathbf{a})$, the conditional mean is computed by $\mu(\bar{\theta}) = \tilde{\mu}_{K'}[\bar{\theta}] / n_{K'}[\bar{\theta}]$.

c) The term $\sum_{\mathbf{c} \in \Omega(\bar{\theta})} \left(\sum_{i \in \mathcal{I}} \sqrt{\rho}\psi_i c_i \right)^2$ is calculated by sequentially implementing

$$\vartheta_k[\bar{\theta}] = \sum_{\tau=0, \dots, 2^m-1} \left(\vartheta_{k-1}[\bar{\theta} - a_k\tau] + 2\tau\sqrt{\rho}\psi_k u_{k-1}[\bar{\theta} - a_k\tau] + (\tau\sqrt{\rho}\psi_k)^2 \right).$$

When reaching layer K' , the conditional variance is obtained as

$$\sigma^2(\bar{\theta}) = s_{K'}[\bar{\theta}] / n_{K'}[\bar{\theta}] - \mu^2(\bar{\theta}) + \gamma^2 \bar{\sigma}^2. \quad (34)$$

We emphasize that, even for a LCMA system with an off-the-shelf binary channel code and BPSK/QPSK, the latticed based soft detection algorithm developed in this paper is required.

B. Example with Exact IF

Our developed algorithm applies to any filtering matrix. If exact IF (EIF) is adopted in a $K \leq N$ system, the filter is given by [27] $\mathbf{W}_{RIF} = \mathbf{A} (\mathbf{H}^T \mathbf{H})^{-1} \mathbf{H}^T$. The signal is then given as

$$\bar{y}_l = \sum_{i \in \mathcal{I}_l} \sqrt{\rho}\psi_{l,i} c_i + \bar{z}_l = \sum_{i \in \mathcal{I}_l} \sqrt{\rho} a_{l,i} c_i + \bar{z}_l. \quad (35)$$

The last equality follows from that $(\mathbf{H}^T \mathbf{H})^{-1} \mathbf{H}^T \mathbf{H} = \mathbf{I}$. In this case, the effective gains are exactly identical to the coefficient vectors. Thus, $\mu_l(\bar{\theta}) = \bar{\theta}$ and $\sigma_l^2(\bar{\theta}) = \gamma^2 \bar{\sigma}_l^2$, which are utilized in (30) to calculate the APP of ICB. The a priori probabilities are required to be calculated as in (32).

C. Example with Regularized IF (Detection Method III)

EIF does not support an MA setup of $K > N$, and suffers from loss particularly at low SNR. Regularized IF (RIF) can address the above issues, whose filter matrix is [27]

$$\mathbf{W}_{RIF} = \mathbf{A}\mathbf{H}^T (\rho\mathbf{H}\mathbf{H}^T + I_N)^{-1}. \quad (36)$$

With \mathbf{W}_{RIF} , the signal can be written as

$$\bar{y}_l = \sum_{i \in \mathcal{I}_l} \sqrt{\rho} \psi_{l,i} c_i + \bar{z}_l = \sum_{i \in \mathcal{I}_l} \sqrt{\rho} a_{l,i} c_i + e_l. \quad (37)$$

The estimation error term is

$$e_l = \sum_{i \in \mathcal{I}_l} \sqrt{\rho} (\psi_{l,i} - a_{l,i}) c_i + \bar{z}_l. \quad (38)$$

Different from EIF, here the error term e_l is correlated with the useful signal part $\sum_{i \in \mathcal{I}_l} \sqrt{\rho} a_{l,i} c_i$. This leads to $\mu_l(\bar{\theta}) \neq \bar{\theta}$ and $\sigma_l^2(\bar{\theta}) \neq \gamma^2 \tilde{\sigma}_l^2$, which should be calculated as in (28) and (29), respectively.

For a sufficiently large K , the number of terms that adds up in (38) is sufficiently large to apply Central Limit Theorem for e_l . Hence, one may approximate e_l as a Gaussian random variable with variance $E(e_l^2)$. It can be easily shown that the MSE of e_l has a close-form representation

$$E(e_l^2) = \gamma^2 \mathbf{a}_l^T (\rho\mathbf{H}^T\mathbf{H} + \mathbf{I})^{-1} \mathbf{a}_l^T. \quad (39)$$

Further, by disregarding the bias in the estimation error term, the mean of e_l is approximated as zero. As such, the calculation of the APP in (30) is further simplified into

$$p(v_l = \theta | \bar{y}_l) \approx \frac{1}{\eta} \sum_{\bar{\theta}: \mathbf{a}_l^T \otimes \mathbf{c} = \theta} \exp\left(-\frac{(\bar{y}_l - \bar{\theta})^2}{2E(e_l^2)}\right) p(\bar{\theta}). \quad (40)$$

This is referred to as *Detection Method III*, which is inferior to Detection Method II due to the approximation in the conditional mean and variance. Note that the a priori probabilities are required to be calculated as in (32), while the calculations of conditional means and variances are avoided.

For a relatively small value of K , Detection Method II is suggested where the loss of Method III may be considerable. For a large K , either Method II or Method III could be used. The receiver's processing with linear LCMA detection method III is summarized in Algorithm 1.

Algorithm 1 Summary of LCMA Detection and Decoding

- Step 1) Calculate the filtering matrix \mathbf{W}_{RIF} according to (36). Perform the filtering process (37).
- Step 2) Calculate the MSE $E(e_l^2)$ according to (39) for $l = 1, \dots, K$.
- Step 3) Perform (40) in parallel to calculate the APPs $p(v_l = \theta|\bar{y}_l)$ for the K streams of codeword-level ICBs. Forward the K streams APPs to the K ring-code decoders.
- Step 4) Perform ring-code decoding for the K streams, which yields the decisions on $\mathbf{u}_1, \dots, \mathbf{u}_K$.
- Step 5) Recover K users' messages by implementing $\mathbf{B} = \tilde{\mathbf{A}}^{-1} \otimes \mathbf{U}$.
-

VI. ON THE OPTIMIZED DESIGN OF UPLINK LCMA

A. Optimized Coefficient Matrix \mathbf{A}

In this section, we focus on LCMA with linear detection and provide a efficient yet powerful suboptimal solution to⁵ \mathbf{A} . Following the convention in studying uplink MA, we consider that all users have symmetric rate. Our development can be extended to non-symmetric rates. For a realization of \mathbf{H} , let the MMSE matrix be denoted by $\Psi = (\rho\mathbf{H}^T\mathbf{H} + \mathbf{I}_K)^{-1}$. Its eigen-decomposition is

$$\Psi = \mathbf{V}\mathbf{D}\mathbf{V}^T. \quad (41)$$

The rate for reliable communication of LCMA is characterized as in the following theorem.

Theorem 2: A symmetric rate R_0 is achievable if there exists K integer vectors $\mathbf{a}_1, \dots, \mathbf{a}_K$, that are linearly independent in \mathbb{Z}_{2^m} , such that

$$\mathbf{D}^{\frac{1}{2}}\mathbf{V}^T\mathbf{a}_l < \sqrt{\frac{1}{2^{2R_0}}}, \forall l = 1, \dots, K. \quad (42)$$

Proof. [Proof of Theorem 2] : It can be shown that the MSE in the linear estimator of $\mathbf{a}_l^T \mathbf{x}[t]$ is

$$\min_{\mathbf{w}_l} E \left(|\mathbf{w}_l^T \mathbf{y}[t] - \mathbf{a}_l^T \mathbf{x}[t]|^2 \right) = \mathbf{a}_l^T (\rho\mathbf{H}^T\mathbf{H} + \mathbf{I}_K)^{-1} \mathbf{a}_l = \mathbf{a}_l^T \mathbf{V}\mathbf{D}\mathbf{V}^T \mathbf{a}_l. \quad (43)$$

As n tends to infinity, the effective noise sphere is given by such MSE for computing the l th ICB. There exist a nested lattice-code with simultaneous ‘‘Roger-goodness’’ and ‘‘Poltyrev-goodness’’, such that the rate

$$R_l^{comp} = \frac{1}{2} \log_2^+ \left(\frac{1}{\mathbf{a}_l^T \mathbf{V}\mathbf{D}\mathbf{V}^T \mathbf{a}_l} \right). \quad (44)$$

w.r.t. the l th ICB is achievable [23], [27]. The overall achievable symmetric rate is given by

$$R_0 \leq R_{sym} = \min_{l=1, \dots, K} R_l^{comp} = \min_{l=1, \dots, K} \frac{1}{2} \log_2^+ \left(\frac{1}{\mathbf{a}_l^T \mathbf{V}\mathbf{D}\mathbf{V}^T \mathbf{a}_l} \right).$$

⁵The optimized \mathbf{A} here is not optimal for the non-linear soft detectors, but also works reasonably well therein.

Then, all K ICBs can be reliably computed if

$$\min_{l=1,\dots,K} \frac{1}{2} \log_2^+ \left(\frac{1}{\mathbf{a}_l^T \mathbf{V} \mathbf{D} \mathbf{V}_l^T \mathbf{a}} \right) > R_0, \quad (45)$$

then all users' messages can be recovered. As (45) is equivalent to (42), the proof is completed. ■

Given Theorem 2, the problem is now to find K linearly independent lattice points, formed by the basis $\mathbf{D}^{\frac{1}{2}} \mathbf{V}^T$, within the boundary of radius $\sqrt{\frac{1}{2^{2R_0}}}$. This is referred to as a *bounded independent vectors problem* (BIVP). Solving BIVP is easier than solving the shortest independent vector problem (SIVP), as one only need K independent points within the radius $\sqrt{\frac{1}{2^{2R_0}}}$ rather than the K shortest ones. The linear independence of $\mathbf{a}_1, \dots, \mathbf{a}_K$ is w.r.t. \mathbb{Z}_{2^m} , which guarantees that $\tilde{\mathbf{A}} = \text{mod}(\mathbf{A}, 2^m)$ has a unique inverse in \mathbb{Z}_{2^m} . For a relatively large K and m , the linear independence w.r.t. \mathbb{Z}_{2^m} is equivalent to that in \mathbb{Z} in probability. We now propose a *rank-constrained sphere decoding* (RC-SD) algorithm which solves the BIVP in (42). The goal is to find K coefficient vectors $\mathbf{a}_1, \dots, \mathbf{a}_K$ that are 1) within the boundary of radius $\sqrt{\frac{1}{2^{2R_0}}}$ and 2) has full-rank K . In RC-SD, we start with an initial radius that is smaller than $\sqrt{\frac{1}{2^{2R_0}}}$ and apply sphere decoding tree search. If the rank for the candidates within the boundary is smaller than K , the radius is added by a certain small step and continue the tree search, until the rank reaches K . Then, we pick those K linearly independent vectors with smallest norms. A pseudo code is given in Algorithm 2 in Appendix.

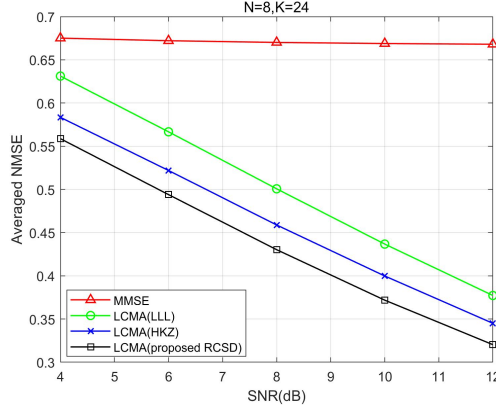


Fig. 2. Averages NMSE with the proposed RS-SD, $N = 8, K = 24$. The channel coefficients follows Rayleigh distribution.

Fig. 2 shows the averaged normalized MSE (NMSE) w.r.t. the ICBs where $N = 8, K = 24$, i.e., the system load of LCMA is 300%. It is well-known that NMSE characterizes the quality of the soft detection output. The smaller the NMSE, the greater the mutual information or supported code rate, following the notion of sphere-packing [47]. The conventional non-lattice-coded based scheme

with MMSE detection fail to support this system load, as the MSE barely drops as SNR increases. In contrast, the LCMA scheme, with any of the three methods for obtaining coefficient matrix \mathbf{A} , can support the system load of 300%. In particular, our proposed RC-SD method considerably outperforms existing LLL and HKZ lattice reduction methods [31]. We note that the efficiency of RC-SD algorithm may be further improved by jointly considering the full-rank condition in reducing the dimension of the search space, which will be investigated in the future.

LCMA is different from lattice-reduction based MIMO detection [31]. LCMA utilizes n -dimension RCM as the underlying coding-modulation, where the lattice is characterized by the generator matrix \mathbf{G} . The optimization of LCMA is based on the lattice obtained from the MMSE matrix. Lattice-reduction based MIMO detection is dealing with the lattice generated by the channel matrix \mathbf{H} .

B. Optimized Spreading Signature Sequences $\mathbf{s}_1, \dots, \mathbf{s}_K$

Since the identification of \mathbf{A} is solved, we are now in the position to study the optimized spreading signature sequences $\mathbf{S} = [\mathbf{s}_1, \dots, \mathbf{s}_K]$ of LCMA. Consider a deterministic channel with a single-antenna (or a single-beam), e.g. an AWGN MA channel, the signal model can be represented by

$$\mathbf{Y} = \sqrt{\rho}\mathbf{S}\mathbf{X} + \mathbf{Z}. \quad (46)$$

The achievable rate is a function of \mathbf{S} and \mathbf{A} . The joint optimization of $\{\mathbf{S}, \mathbf{A}\}$ is very difficult. We suggest a pragmatic method that decouples the optimization of \mathbf{S} and \mathbf{A} as follows:

First, solve the optimization of \mathbf{S} for a given \mathbf{A} , formulated as

$$\begin{aligned} & \arg \max_{\mathbf{S}} \sum_{l=1}^K \frac{1}{2} \log_2^+ \left(\frac{1}{\mathbf{a}_l^T (\rho \mathbf{S}^T \mathbf{S} + \mathbf{I}_K)^{-1} \mathbf{a}_l} \right) \\ & \text{s.t. } \text{Tr} \{ \mathbf{S}^T \mathbf{S} \} \leq K \quad \forall i = 1, \dots, K \end{aligned} \quad (47)$$

where a total power constraint is considered. The formulation w.r.t. individual power constraint just needs to modified the constraint into $\mathbf{s}_i^T \mathbf{s}_i \leq 1$. The max-min is replaced by the max-sum in (47), which is implementable in SD. This can be approximately solved by using a steepest descend (SD) algorithm. The Pseudo code is presented in Algorithm 3 in Appendix. Next, for the given \mathbf{S} , solve the optimization of \mathbf{A} as in (42) (\mathbf{H} replaced by \mathbf{S}) with the RC-SD algorithm. Then, carry out iterations between the above two steps until convergence. This paper devotes no efforts to rigourously prove the optimality of this pragmatic solution. As the optimization of the spreading sequences \mathbf{S} is off-line, one may assign various initial values of \mathbf{S} (or \mathbf{A}) and select the one with the best rate.

Fig. 3 presents the achievable symmetric rate of LCMA in an AWGN MA channel, using the spreading matrix optimized above. Here we present with $N = 8$, $K = 16, 24$. For SNR greater than 4 dB, the difference between the achievable symmetric rate of LCMA and that of the upper bound (UB) of the MA channel capacity is almost unnoticeable for $K=16$, and is quite small (about 0.05 bit) for $K=24$. At low SNRs, the gap becomes greater. This is due to the well-known inherent loss of the lattice-code based scheme that achieves $\frac{1}{2} \log^+ (\varkappa + SNR)$, with $\varkappa < 1$ in general [23], [24].

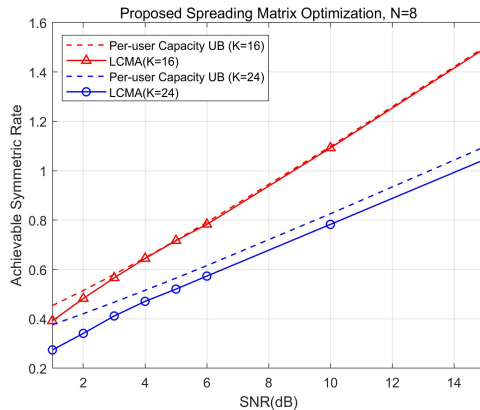


Fig. 3. Achievable symmetric rate of LCMA with the proposed spreading matrix \mathbf{S} , AWGN MA channel, $N = 8$, $K = 16$ and 24 .

VII. NUMERICAL RESULTS

A. AWGN MA Channel

Fig. 4 shows the BER of LCMA for AWGN MA channel with spreading length $N_S = 8$, $K = 16$ and 24 users. Each user utilizes BPSK and a rate $1/2$ binary irregular repeat accumulate (IRA) code of length $k = 65536$, where the utilization of a long channel code is for the sake of comparison to the capacity limit. The IRA code is from that in [6] optimized for single-user point-to-point AWGN channel. The system loads for $K=16$ and 24 are 200% and 300%, translated into per-chip spectral efficiency of 1 and 1.5 bits per real dimension respectively. The spreading matrix of LCMA is obtained using Algorithm 3 given in Appendix. Detection Method II is utilized with which the receiver computes the APPs of the ICBs over the lattice.

The capacity limit UB of the MA channel and rate limit of LCMA are also drawn. For $K = 16$, at BER of 10^{-4} , the performance is about 0.71 dB and 1.04 dB away from the rate limit of LCMA and MA capacity UB, respectively. For $K = 24$, the performance is about 0.69 dB and 1.39 dB away from the rate and capacity limits. These are in line with the achievable rate in Fig. 3.

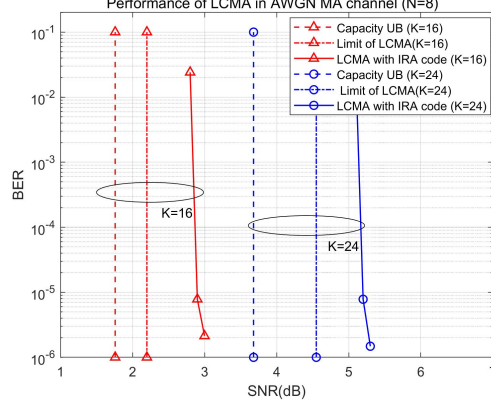


Fig. 4. BER of LCMA in AWGN MA channel with spreading length $N_S = 8$, $K = 16$ and 24 users. Each user utilizes BPSK and a rate 1/2 IRA code of length $k = 65536$. The per-chip spectral efficiency is 1 and 1.5 bits per real dimension.

Fig. 5 shows the FER of LCMA with $N_S = 8$ and $K = 16, 20, 24$, where a rate 1/2 length-1920 LDPC code in 5G standard and BPSK are used. Detection Method I and II are used for $K = 20$, and Method III is used for $K = 24$. For $K = 20$, it is shown that lattice-based MA with Detection Method I based on MD-PNC exhibits a 0.9 dB gain over that with Detection Method II based on RIF. This is due to that MD-PNC utilizes the intact N -dimension space to calculate the ICB, avoiding the loss over linear filtering process of RIF that may overly compressed the signal space.

We also compare to existing non-lattice based IDMA system with chip-level interleaving and iterative elementary signal estimation (ESE) detection, and SCMA system with iterative message passing detection and decoding⁶. All schemes have identical power among K users, where the spreading matrix of LCMA has entries in $\{-1, 0, +1\}$ as given in Table II with column-wise normalization, see Appendix. It is observed that LCMA can support all system loads evaluated. In contrast, IDMA and SCMA fail to support a system load greater than 200%. This is due to the poor adaptation of the 5G LDPC code with the ESE or message passing detector, following the principle of EXIT chart for the convergence behavior of the iterative detection and decoding (IDD). Due to the nature of parallel processing of LCMA, the stronger the underlying channel code is, the better the performance. We note that such competitive performance is achieved with merely parallel processing and K single-user decoding, without using successive cancelation or IDD.

⁶We do not include comparison to RSMA, as it is for the close-loop MA system where extensive rate allocation is employed [16]. We do not include PDMA, MUSA and etc. for comparison, as their mechanisms are not largely different to IDMA and SCMA.

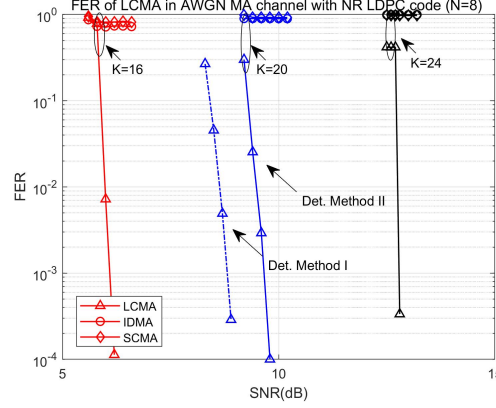


Fig. 5. BER of LCMA in AWGN MA channel with $N_s = 8$. BPSK and a rate 1/2 LDPC code of length $k = 1920$ are utilized.

B. Fading MA Channel

We next consider fading MA channel, where the fading coefficients remains unchanged within a coded block and varies over blocks. Our developed techniques can be extended to time-varying or frequency-selective channels following the treatments as in ring CF [33] and multi-mode IF [32]. The extension to asynchronous MA can be treated as in the asynchronous PNC [48]. Fig. 6 shows the FER of LCMA where $K = 10, 14, 16$ and $N_s = 4$. A rate 1/2 length-480 LDPC code is used. The spreading sequences of LCMA are given in Table II in Appendix. $Q = 10$ receiver iterations are implemented in IDMA and SCMA. It is observed that LCMA outperforms baseline schemes in supported system load as well as in FER. IDMA and SCMA fail to support $K = 16$ users, while they can hardly achieve FER below 10^{-1} or 10^{-2} for $K = 14$ users and $K = 10$ users, respectively.

C. MU-MIMO

We next consider the MU-MIMO setup where the receiver is equipped with N_R antennas. In this setting, the iterative ESE or BP algorithms are implemented in the form of an iterative linear MMSE soft cancellation algorithm: the signal of each received antenna can be viewed as a chip-level signal in IDMA/SCMA; the chip-level cancelation with elementary extrinsic information feedback is conducted; the linear MMSE filtering combines all N_R received antennas signals. Fig. 7 shows the FER of LCMA where $N_R = 8$ and $K = 16, 20, 24$. BPSK and a length-480 5G NR LDPC code of rate 1/2 are utilized. $Q = 10$ receiver iterations are implemented in iterative MMSE detection. It is

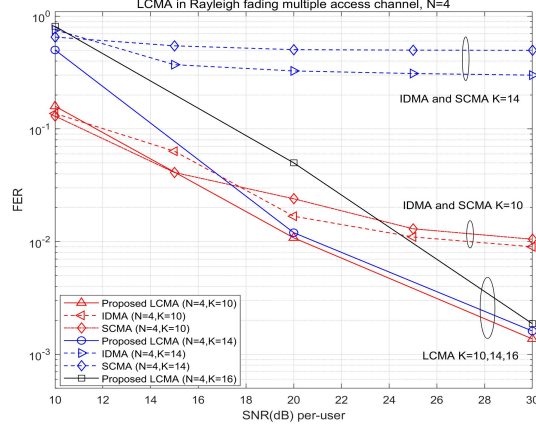


Fig. 6. FER of LCMA with various system loads in Rayleigh fading MA channel.

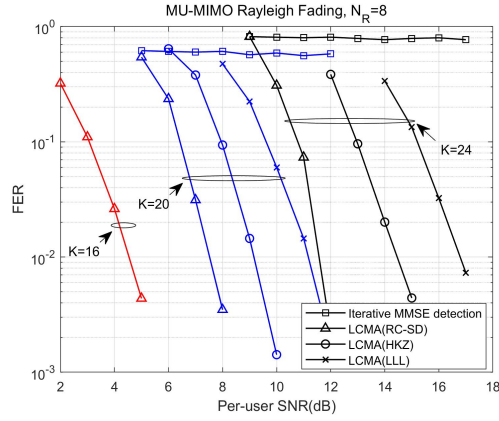


Fig. 7. FER of LCMA in multi-user MIMO of $N_R = 8$ receive antennas. LCMA can support a system load of no less than 300%, while the baseline scheme with iterative receiver cannot support a load greater than 200%. Detection Method III is used for $K = 24$.

clear that LCMA can support a system load of no less than 300%, while the baseline scheme with iterative receiver cannot support a system load greater than 200% where the FER curve flats out.

We next consider MA with higher level modulations, e.g., 2^m -PAM (or 2^{2m} -QAM). Each user utilizes the 2^m -ary ring code for encoding (1) and mapped to 2^m -PAM. Fig. 8 shows the FER of LCMA with $m = 2$ (4-PAM), $N_R = 4$, $K = 8$. The information rate is 8 bits per channel-use per real dimension. Here we utilize a doubly irregular repeat accumulate (D-IRA) code over integer ring $\{0, 1, 2, 3\}$ with coding rate 1/2 in the LCMA system [42]. It is demonstrated that for 4-PAM, LCMA can support a system load of at least 200% with just parallel processing. In contrast, iterative MMSE detection with 4-PAM fails to converge at this system load. It is also observed that Detection

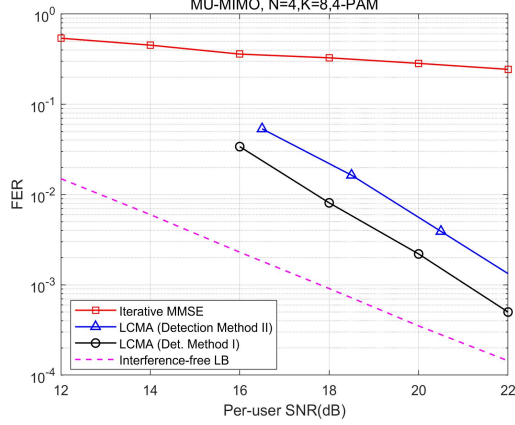


Fig. 8. FER of LCMA with 4-PAM in MU-MIMO, $N_R = 4$, $K = 8$. The list size of Detection method I is set to 100. For 4-PAM, LCMA can support a system load of at least 200%, while iterative MMSE detection fails to converge.

method I with MD-PNC outperforms Detection method II with RIF by about 0.89 dB. This again supports the superiority of the newly developed non-linear soft detection algorithm. We again note that a 2^m -ary ring-code is required in LCMA for 4-PAM. Existing schemes such BICM and TCM are not lattice codes hence does not support the LCMA processing. The details on the design of 2^m -ary ring-codes can be found in [42].

TABLE I
THE ORDERS OF COMPLEXITIES OF LCMA, IDMA AND SCMA SYSTEMS

	Detection	Decoding	Coefficient Identification	Interleaver&De-interleaver
LCMA	$O(Knq \cdot E(\omega_H(\mathbf{a})))$ for Det. Method II and III, $O(Kn \mathcal{L})$ for Method I	$O(Kn(q-1))$	Between $O(K^3)$ and $O(K^4)$	not required
IDMA	$O(Q \cdot Kn \log_2^q \cdot N_S)$	$O(Q \cdot Kn \log_2^q)$	not required	$O(2Q \cdot Kn \cdot N_S)$
SCMA	$O(Q \cdot K^2 n \log_2^q)$	$O(Q \cdot Kn \log_2^q)$	not required	$O(2Q \cdot Kn)$

D. Analysis of Implementation Costs of LCMA

The orders of complexities are shown in Table. I. The typical value of receiver iterations Q is between 4 to 10 for IDMA/SCMA. The computation in LCMA consists of 1) channel-code decoding, 2) LCMA soft detection, and 3) identification of \mathbf{A} . For 1), LCMA requires only K decoding operations while IDMA/SCMA requires Q times more. For the uplink MA, the modulation order $q = 2^m$ is usually not large, where the complexity of ring-code decoding is not considerably greater than that based on binary channel code decoding.

For 2), LCMA needs to compute K streams of APPs w.r.t. the ICBs, while IDMA/SCMA requires to compute $Q \cdot K$ streams of soft estimates. In particular, if Detection methods II or III is utilized, the per-symbol detection complexity (of calculating the distance and the likelihood function) of stream l is of order $O((q-1)\omega_H(\mathbf{a}_l))$, where $\omega_H(\mathbf{a}_l) < K$ denotes the weight of the coefficient vector \mathbf{a}_l . The average detection complexity of LCMA is thus $O(Kn(q-1)E(\omega_H(\mathbf{a})))$. In contrast, the iterative chip-by-chip detection of IDMA has a complexity of $O(Q \cdot Kn \log_2^q N_S)$, while that of SCMA is $O(Q \cdot Kn \log_2^q E(\omega(\mathbf{s})))$ where $E(\omega(\mathbf{s}))$ denotes the average number of non-zero entries of the spreading sequence \mathbf{s} . Due to the avoidance of iterative detection, the overall detection complexity of LCMA is smaller than that of IDMA/SCMA.

For 3), with LLL, the complexity is between $O(K^3)$ and $O(K^4)$, a polynomial in K . The complexity of HKZ and RC-SD is moderately higher than LLL. Since \mathbf{A} is chosen once per block, for a moderate-to-long block length n (e.g. $n > 480$), this overhead is not significant.

VIII. CONCLUSIONS

This paper studied lattice-code based MA. We developed a package of techniques essential to its practical implementation, including the 2^m -ary ring-coded modulation, LCMA soft detection algorithms, rate-constrained sphere-decoding for solving the BIVP that identifies the optimized coefficient matrix \mathbf{A} , and a pragmatic solution for optimizing the MA spreading matrix \mathbf{S} . The per-user detection complexity is of order no greater than $O(K)$, suitable for massive access. Our proposed new non-linear LCMA detection algorithm with MD-PNC outperforms linear detection such as regularized IF. Considerable system load and error rate performance enhancement were demonstrated over existing schemes, without successive interference cancellation of iterative detection and decoding. Off-the-shelf binary codes such as 5G NR LDPC codes can be directly used in LCMA for any system load, avoiding the issue of adaptation of channel-code and multi-user detector.

REFERENCES

- [1] W. Tong and P. Zhu, "6G the next horizon—from connected people and things to connected intelligence," *Cambridge University Press*, 2021.
- [2] D. Tse and P. Viswanath, "Fundamentals of wireless communication," *Cambridge University Press*, 2005.
- [3] L. Dai, B. Wang, Z. Ding, Z. Wang, S. Chen, and L. Hanzo, "A survey of non-orthogonal multiple access for 5G," *IEEE Communications Surveys and Tutorials*, vol. 20, no. 3, pp. 2294–2323, 2018.
- [4] Z. Ding, Y. Liu, J. Choi, Q. Sun, M. Elkashlan, I. Chih-Lin, and H. V. Poor, "Application of non-orthogonal multiple access in LTE and 5G networks," *IEEE Commun. Mag.*, vol. 55, no. 2, pp. 185–191, 2017.
- [5] T. M. Cover and J. A. Thomas, "Elements of information theory," *John Wiley & Sons, Inc.*, 1991.

- [6] S. ten Brink and G. Kramer, "Design of repeat-accumulate codes for iterative detection and decoding," *IEEE Trans. Signal Processing*, vol. 51, no. 11, pp. 2764–2772, 2003.
- [7] S. Ten Brink, "Convergence behavior of iteratively decoded parallel concatenated codes," *IEEE Trans. Comm.*, vol. 49, no. 10, pp. 1727–1737, 2001.
- [8] J. Zhu and M. Gastpar, "Gaussian multiple access via compute-and-forward," *IEEE Trans. Inf. Theory*, vol. 63, no. 5, pp. 2678–2695, 2016.
- [9] S. R. Islam, N. Avazov, O. A. Dobre, and K.-S. Kwak, "Power-domain non-orthogonal multiple access (NOMA) in 5G systems: Potentials and challenges," *IEEE Commun. Surv. Tuts.*, vol. 19, no. 2, pp. 721–742, 2016.
- [10] X. Wang and H. V. Poor, "Iterative (turbo) soft interference cancellation and decoding for coded CDMA," *IEEE Trans. Comm.*, vol. 47, no. 7, pp. 1046–1061, 1999.
- [11] P. Li, L. Liu, K. Wu, and W. Leung, "Interleave division multiple-access," *IEEE Trans. Wireless Comm.*, vol. 5, no. 4, pp. 938–947, Apr. 2006.
- [12] H. Nikopour and H. Baligh, "Sparse code multiple access," in *Proc. IEEE 24th Int. Symp. Pers. Indoor Mobile Radio Commun. (PIMRC)*, pp. 332–336, 2013.
- [13] S. Kudekar and K. Kasai, "Spatially coupled codes over the multiple access channel," in *2011 IEEE International Symposium on Information Theory Proceedings*, pp. 2816–2820, 2011.
- [14] T. Yang, J. Yuan, and Z. Shi, "Rate optimization for IDMA systems with iterative joint multi-user decoding," *IEEE Trans. Wireless Comm.*, vol. 8, no. 3, pp. 1148–1153, Mar. 2009.
- [15] B. Rimoldi and R. Urbanke, "A rate-splitting approach to the Gaussian multiple-access channel," *IEEE Transactions on Inf. Theory*, vol. 42, no. 2, pp. 364–375, 1996.
- [16] Y. Mao, B. Clerckx, and V. O. K. Li, "Rate-splitting for multi-antenna non-orthogonal unicast and multicast transmission: Spectral and energy efficiency analysis," *IEEE Trans. Comm.*, vol. 67, no. 12, pp. 8754–8770, 2019.
- [17] S. Chen, B. Ren, Q. Gao, S. Kang, S. Sun, and K. Niu, "Pattern division multiple access—A novel nonorthogonal multiple access for fifth-generation radio networks," *IEEE Trans. Vehi. Tech.*, vol. 66, no. 4, pp. 3185–3196, 2016.
- [18] Y. Cheng, L. Liu, and L. Ping, "Orthogonal AMP for massive access in channels with spatial and temporal correlations," *IEEE J. Sel. Areas Commun.*, vol. 39, no. 3, pp. 726–740, 2021.
- [19] Z. Sun, Y. Xie, J. Yuan, and T. Yang, "Coded slotted aloha for erasure channels: Design and throughput analysis," *IEEE Trans. Commun.*, vol. 65, no. 11, pp. 4817–4830, 2017.
- [20] E. Paolini, G. Liva, and M. Chiani, "Coded slotted aloha: A graph-based method for uncoordinated multiple access," *IEEE Trans. Inf. Theory*, vol. 61, no. 12, pp. 6815–6832, 2015.
- [21] B. Nazer and M. Gastpar, "Computation over multiple-access channels," *IEEE Trans. Inf. Theory*, vol. 53, no. 10, pp. 3498–3516, 2007.
- [22] R. Zamir, S. Shamai, and U. Erez, "Nested linear/lattice codes for structured multiterminal binning," *IEEE Trans. Inf. Theory*, vol. 48, no. 6, pp. 1250–1276, 2002.
- [23] B. Nazer and M. Gastpar, "Compute-and-forward: Harnessing interference through structured codes," *IEEE Trans. Inf. Theory*, vol. 57, no. 10, pp. 6463–6486, Oct. 2011.
- [24] W. Nam, S. Chung, and Y. H. Lee, "Capacity of the Gaussian two-way relay channel to within 1/2 bit," *IEEE Trans. Inf. Theory*, vol. 56, no. 11, pp. 5488–5494, Nov. 2010.
- [25] X. Yuan, T. Yang, and I. Collings, "Multiple-input multiple-output two-way relaying: a space-division approach," *IEEE Trans. Inf. Theory*, vol. 59, no. 10, pp. 6421–6440, Oct. 2013.
- [26] S. H. Lim, C. Feng, A. Pastore, B. Nazer, and M. Gastpar, "Compute-forward for DMCs: Simultaneous decoding of multiple combinations," *IEEE Trans. Inf. Theory*, vol. 66, no. 10, pp. 6242–6255, 2020.

- [27] J. Zhan, B. Nazer, U. Erez, and M. Gastpar, "Integer-forcing linear receivers," *IEEE Trans. Inf. Theory*, vol. 60, no. 12, pp. 7661–7685, Dec. 2014.
- [28] D. Silva, G. Pivaro, G. Fraidenraich, and B. Aazhang, "On integer-forcing precoding for the Gaussian MIMO broadcast channel," *IEEE Tran. Wireless Comm.*, vol. 16, no. 7, pp. 4476–4488, 2017.
- [29] S.-N. Hong and G. Caire, "Compute-and-forward strategies for cooperative distributed antenna systems," *IEEE Trans. Inf. Theory*, vol. 59, no. 9, pp. 5227–5243, Sep. 2013.
- [30] T. Yang, "Distributed MIMO broadcasting: Reverse compute-and-forward and signal-space alignment," *IEEE Trans. Wireless Comm.*, vol. 16, no. 1, pp. 581–593, 2017.
- [31] A. Sakzad, J. Harshan, and E. Viterbo, "Integer-forcing MIMO linear receivers based on lattice reduction," *IEEE Trans. Wireless Comm.*, vol. 12, no. 10, pp. 4905–4915, 2013.
- [32] D. Yang and K. Yang, "Multimode integer-forcing receivers for block fading channels," *IEEE Transactions on Wireless Communications*, vol. 19, no. 12, pp. 8261–8271, 2020.
- [33] S. Lyu, A. Campello, and C. Ling, "Ring compute-and-forward over block-fading channels," *IEEE Transactions on Information Theory*, vol. 65, no. 11, pp. 6931–6949, 2019.
- [34] O. Ordentlich and U. Erez, "Cyclic-coded integer-forcing equalization," *IEEE Transactions on Information Theory*, vol. 58, no. 9, pp. 5804–5815, 2012.
- [35] E. Sula, J. Zhu, A. Pastore, S. H. Lim, and M. Gastpar, "Compute-forward multiple access (CFMA): Practical implementations," *IEEE Trans. Comm.*, vol. 67, no. 2, pp. 1133–1147, 2018.
- [36] Q. Chen, F. Yu, T. Yang, J. Zhu, and R. Liu, "A linear physical-layer network coding based multiple access approach," in *2022 IEEE International Symposium on Information Theory (ISIT)*, pp. 2803–2808, 2022.
- [37] Q. Chen, F. Yu, T. Yang, and R. Liu, "Gaussian and fading multiple access using linear physical-layer network coding," *IEEE Trans. Wireless Comm.*, early access, 2022.
- [38] N. Sommer, M. Feder, and O. Shalvi, "Low-density lattice codes," *IEEE Trans. Inf. Theory*, vol. 54, no. 4, pp. 1561–1585, 2008.
- [39] M.-C. Chiu, "Bandwidth-efficient modulation codes based on nonbinary irregular repeat-accumulate codes," *IEEE Trans. Inf. Theory*, vol. 56, no. 1, pp. 152–167, 2010.
- [40] M. Qiu, L. Yang, Y. Xie, and J. Yuan, "On the design of multi-dimensional irregular repeat-accumulate lattice codes," *IEEE Transactions on Communications*, vol. 66, no. 2, pp. 478–492, 2018.
- [41] Q. T. Sun, J. Yuan, T. Huang, and K. W. Shum, "Lattice network codes based on eisenstein integers," *IEEE Transactions on Communications*, vol. 61, no. 7, pp. 2713–2725, 2013.
- [42] F. Yu, T. Yang, and Q. Chen, "Doubly irregular repeat modulation codes over integer rings for multi-user communications," *submitted to IEEE Trans. Comm.*, 2022 (available at: <https://shi.buaa.edu.cn/yangtom0403/en/lwgc/32786/content/25308.htm#lwgc>).
- [43] S. Lin and D. J. Costello, "Error control coding, 2nd edition," *Pearson*, 2004.
- [44] T. Yang, L. Yang, Y. J. Guo, and J. Yuan, "A non-orthogonal multiple-access scheme using reliable physical-layer network coding and cascade-computation decoding," *IEEE Trans. Wireless Comm.*, vol. 16, no. 3, pp. 1633–1645, 2017.
- [45] B. M. Hochwald and S. ten Brink, "Achieving near-capacity on a multiple-antenna channel," *IEEE Trans. Comm.*, vol. 51, no. 3, pp. 389–400, Mar. 2003.
- [46] S. H. Lim, C. Feng, A. Pastore, B. Nazer, and M. Gastpar, "A joint typicality approach to compute-forward," *IEEE Trans. Inf. Theory*, vol. 64, no. 12, pp. 7657–7685, 2018.
- [47] U. Erez and R. Zamir, "Achieving $\log(1+\text{SNR})$ on the AWGN channel with lattice encoding and decoding," *IEEE Trans. Inf. Theory*, vol. 50, no. 10, pp. 2293–2314, 2004.

- [48] Q. Yang and S. C. Liew, "Asynchronous convolutional-coded physical-layer network coding," *IEEE Trans. Wireless Comm.*, vol. 14, no. 3, pp. 1380–1395, 2015.

APPENDIX

TABLE II

EXAMPLE OF SPREADING SEQUENCE OF LCMA, $K=20$, $N_S=8$.

1	1	1	0	1	1	1	1	1	1	1	1	1	0	1	1	1	1	1	1
1	-1	1	0	1	1	1	1	1	1	-1	-1	-1	0	-1	-1	-1	-1	-1	-1
1	0	-1	-1	1	-1	1	1	1	-1	1	0	-1	-1	1	-1	1	1	1	-1
1	0	-1	-1	1	-1	1	1	1	-1	-1	0	1	1	-1	1	-1	-1	-1	1
1	-1	1	-1	1	1	1	-1	0	-1	1	-1	1	-1	1	1	1	-1	0	-1
1	-1	1	-1	1	1	1	-1	0	-1	-1	1	-1	1	-1	-1	-1	1	0	1
1	0	-1	0	-1	1	0	1	-1	-1	1	0	-1	0	-1	1	0	1	-1	-1
1	0	-1	0	-1	1	0	1	-1	-1	-1	0	1	0	1	-1	0	-1	1	1

Algorithm 2 Rank-constrained Sphere Decoding for identifying \mathbf{A}

Step 1) Set the radius to $r = \sqrt{\frac{1}{2^{2R_0}} - \varepsilon}$. The initial value can be set exoterically.

Step 2) Implement the Cholesky factorization on \mathbf{VDV}_i^T , and apply a tree-search method which finds all candidates \mathbf{a} that are within distance r to the origin.

Step 3) If the rank of the candidates in \mathbb{Z}_{2^m} is less than K . Increase the radius r by a certain (small) step and Go to Step 1). Otherwise, continue to Step 4).

Step 4) Arrange the candidates with a ascending order according to their lengths. Start with the first candidate, use a greedy method to find K coefficient vectors, until the rank in \mathbb{Z}_{2^m} reaches K .

Algorithm 3 Steepest Descent for Optimal \mathbf{S}

Step 1) Set the Lagrangian term $y(\mathbf{S}, u) = \text{tr}(\mathbf{A}^T(\rho\mathbf{S}^T\mathbf{S} + \mathbf{I}_K)^{-1}\mathbf{A}) + u(\text{tr}(\mathbf{S}^T\mathbf{S}) - K)$, u is an intermediate variable.

Calculate the derivatives of the cost function in w.r.t. \mathbf{S} .

Step 2) Update $\mathbf{S} = \mathbf{S} - \alpha(2u\mathbf{S} - 2\rho\mathbf{S}(\rho\mathbf{S}^T\mathbf{S} + \mathbf{I}_K)^{-1}\mathbf{A} \cdot \mathbf{A}^T(\rho\mathbf{S}^T\mathbf{S} + \mathbf{I}_K)^{-1})$, α is the sampling value of a hyperbolic tangent function.

Step 3) Update $u = u + \alpha(\text{tr}(\mathbf{S}^T\mathbf{S}) - K)$.

Step 4) Increase α by a small step and Go to step 2), until \mathbf{S} is stabilized.
